# Mathematical Simulation of Cerebral Blood Flow in Focal Ischemia

ANTAL G. HUDETZ, PH.D., JAMES H. HALSEY, JR., M.D., CHARLES R. HORTON, PH.D., KARL A. CONGER, PH.D., DANIEL D. RENEAU, PH.D.

**SUMMARY** **A computer model was developed to describe regional cerebral blood flow and tissue oxygenation with autoregulation during focal ischemia produced by occlusion of the middle cerebral artery (MCA). This steady state model described the distribution of blood flow in the cerebral arterial system including the circle of Willis as well as the pial arterial anastomoses, and included a simplified form of autoregulation based on the local control of pressure and flow in the pial and intracerebral arteries, respectively. Preliminary simulation studies with the model yielded the following results. Less effective autoregulation was predicted by the model at low blood pressure in focal ischemia. Passive dilatation of the pial vasculature produced a leftward shift in the autoregulatory curve. Simulations with occlusion of the MCA revealed the ultimate importance of the pial anastomoses in providing adequate blood and oxygen supply in the ischemic territories including the specially vulnerable lenticulostriate area. The volume of the ischemic ($pO_2 < 1$ mmHg) brain tissue in the MCA-cortex estimated by using a concurrent Krogh cylinder model was 50% when the pial anastomoses were 80 $\mu$m in diameter and the ischemic area disappeared at 170 $\mu$m diameter. With relatively small anastomoses (< 200 m) the model demonstrated intracerebral steal during intracerebral vasodilation. Passive dilation of the pial arteries including the pial anastomoses caused the steal to disappear and to reverse. These results suggest that both autoregulatory shift and steal reversal can be explained by passive dilatation of the pial vasculature.**

**Stroke**, Vol 13, No 5, 1982

EXPERIMENTAL OBSERVATIONS suggest that a general determinant of the severity of acute cerebral ischemia in response to occlusion at the middle cerebral artery (MCA) is the competence of the collateral circulation.[1-4] During obstruction of the MCA, the majority of the ipsilateral hemisphere can receive blood flow only through the pial anastomoses from the branches of the anterior and posterior cerebral arteries. Similarly, retrograde flow through the lenticulostriate branches of the MCA supplies the internal brain structures (caudate nucleus, putamen, etc.) via the same pial anastomoses. Experimental evidences support that the severity of ischemia in this region plays a central role in the outcome of the ischemic brain injury.[1, 2]

Other studies revealed that in response to strong cerebrovascular vasodilators such as high arterial $pCO_2$, blood flow is "stolen" from the ischemic territory but that the "steal" can be reversed after several hours of MCA occlusion.[3] It is well known that in chronic hypertension the autoregulatory curve shifts, presumably as a result of chronic adaptation of the pial arteries. One wonders if the reversal of the steal phenomenon could also be the consequence of a similar adaptation of the pial arteries and anastomoses to reduced blood or oxygen supply in focal ischemia.

These qualitative speculations about experimental and clinical observations imply mechanisms which are incorporated with a conceptual model or hypothesis: that the pial collateral circulation is of central importance in the adaptation to focal ischemia as well as in the adjustment of autoregulation to sustained blood pressure changes. One way to test this or any hypothesis is to do more laboratory experiments, as we have in progress. Another important test of a hypothesis is to analyze it for its internal consistency. The essential intellectual discipline required is the reduction of qualitative thoughts to mechanisms which can be quantified. These can then be related to each other in a computer simulation, thereby testing the hypothesis with the best available experimental data. If this simulation yields results which seem reasonable according to order of magnitude the hypothesis is thereby somewhat strengthened, while if the order of magnitude is unreasonable this would imply a defect in the hypothesis which then should be changed. Moreover, the intellectual discipline imposed in building the simulation readily identifies areas where more experimental observations are needed.

With preliminary development of our model to be presented in this paper, we have used it to test our hypothesis with the following question: (1) What is the quantitative relationship between regional blood flow or oxygen supply in the ischemic regions and the diameter of anastomoses during MCA occlusion? (2) Is it possible to explain the reversal of cerebral steal by chronic dilation of the pial anastomoses? (3) Is there a common explanation for autoregulatory shift and steal reversal?

A mathematical model was formulated to describe steady flow within the system of cerebral vessels comprising the main arteries of the circle of Willis, the series-coupled peripheral segments and the secondary loops of anastomotic connections between the distal anterior, middle and posterior cerebral arteries. Regional cerebral autoregulation, an important feature not found in earlier cerebral hemodynamic models, was included in the simulation. At different blood flow rates, distribution of oxygen partial pressure in the cerebral tissue was calculated using a modified Krogh

From: Department of Neurology and Pathology and the Stroke Research Center, University of Alabama in Birmingham, Birmingham, Alabama 35294. Supported by Research Grant NO. NS08802.

Address for correspondence: Antal G. Hudetz, Ph.D., Experimental Research Department and 2nd Institute of Physiology, Semmelweis Medical University, Budapest, Ulloi ut78/a, H-1082, Hungary.

Received: August 26, 1981, accepted May 11, 1982.

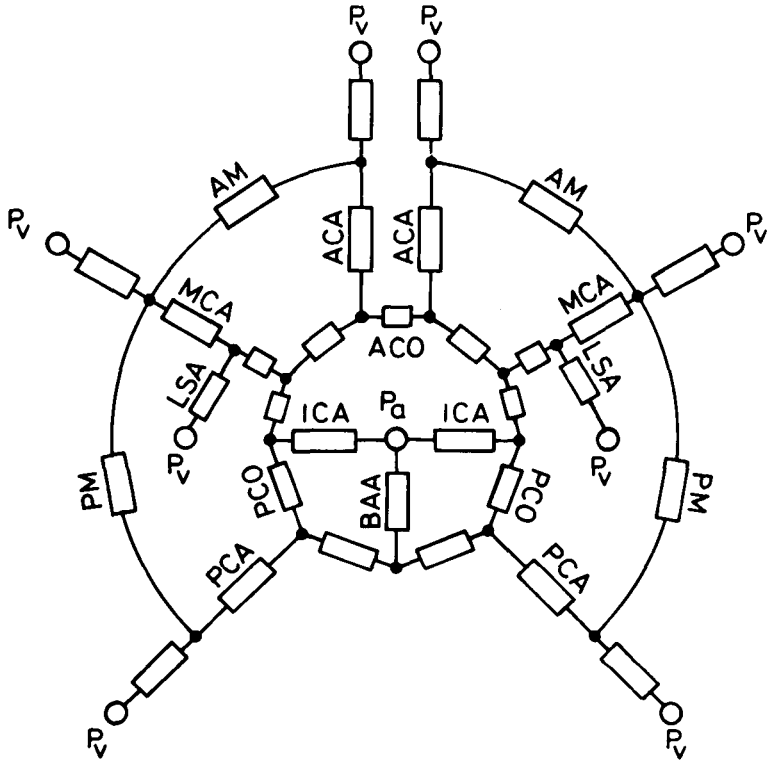


FIGURE 1. *Schematic diagram of the cerebrovascular model. ICA = internal carotid artery, BAA = basilar artery, ACA = anterior cerebral artery, MCA = middle cerebral artery, PCA = posterior cerebral artery, LSA = lenticulostriate arteries, ACO = anterior communicating artery, PCO = posterior communicating artery, AM = antero-medial anastomoses, PM = posteromedial anastomoses, $P_a$ = arterial pressure, $P_v$ = venous pressure.*

cylinder model. Thus, dependence of regional cerebral blood flow and oxygen supply on the pial collateral circulation during focal ischemia produced by long-term MCA occlusion could be studied.

## Description of the Model

The hemodynamic model consisted of the two internal carotid arteries (ICA), the basilar artery (BAA), the circle of Willis, the anterior (ACA), middle (MCA) and posterior (PCA) cerebral arteries, and the lenticulostriate (LSA) arteries. A schematic diagram of the model is displayed in figure 1. Pial anastomotic connections between the main cortical arteries were represented by lumped segments (AM & PM) connecting the anterior and posterior cerebral arteries to the middle cerebral artery respectively. Branches of the ACA, MCA, and PCA were lumped into preanastomotic (pial) and postanastomotic (intracerebral) segments. The postanastomotic segments also included the capillaries and veins. The lenticulostriate vessels were lumped into a single vessel segment.

The model thus comprised 32 vessels and lumped segments connected to each other at 17 branch points. In order to determine hydrodynamic resistance of the vessels, diameter and length measurements of the major cerebral arteries were performed on several monkey brains perfused with formalin at normal arterial pressure. Cerebral arterial casts were also prepared by infusion of plastic* with subsequent corrosion of the brain in concentrated HCl. Although the fixation technics might have altered somewhat the luminal diameters, the more important ratios of diameters were probably not influenced significantly. Diameters and lengths of the vessels used for computer simulation are shown in table 1. For vessels having definite length, hydrodynamic reistance was calculated by $R = 8 \eta L/\pi r^4$ ($\eta$ = 3.0 cp). Hydrodynamic resistance of the lumped pial arteries was set equal to 26% of the total cerebrovascular resistance (CVR), while that of the postanastomotic vessels was set equal to 57% of CVR.[4] The CVR of the monkey was calculated from an arterial pressure of 120 mmHg and a total cerebral blood flow of 25 ml/min.

Lengths of the basilar and internal carotid arteries listed in Table 1 are not physiological but effective lengths, which were adjusted to achieve 17% of the total CVR for the large arteries.[5] In steady flow models it is not the individual values of length and diameter but their ratio $L/r^4$ (i.e. the resistance) that is impor-

TABLE 1 *Geometrical Data of the Cerebral Arterial Segments of the Monkey*

| Arterial segment | Diameter/mm | Length/mm |
|---|---|---|
| Internal Carotid | 1.1 | 170.0* |
| Basilar | 0.8 | 170.0* |
| Anterior Cerebral | 0.6 | 8.0† |
| Middle Cerebral | 0.8 | 1.0† |
| Posterior Cerebral | 0.7 | 4.0† |
| Lenticulostriate | 0.2 | — |
| Anterior Communicating | 0.2 | 1.0 |
| Posterior Communicating | 0.2 | 5.0 |

*Effective lengths.
†Length of the proximal segment.

*Batson's #17 Anatomical corrosion compound diluted 2:1 with J.B. 4 solution a. (Polyscience, Inc.)

tant. The resistance value assigned to the large arteries was obtained in cats,[5] and is likely greater than that of the monkey due to the carotid rete. For monkeys, however, we found no adequate data in the literature.

Since pial anastomotic vessels form a complex network on the cortical surface, an effective length was assigned to these segments as well. The average number of the anastomotic vessels (7 between ACA and MCA), and 4 between PCA and MCA) was included in the calculation of the resistance.[6]

Autoregulation of flow in the cerebrovascular model was based on the integral control of local perfusion pressure and flow in the pial and intracerebral segments. Pial arteries play an important role in autoregulation during alterations in arterial blood pressure.[5,7] Therefore, resistance of the preanastomotic (pial) segments was controlled by the pressure at the outlet of these segments. This idea was suggested by the theory of sequential myogenic control;[8] however, the specific mechanism of the control is not defined explicitly in the present work. Postanastomotic (intracerebral) resistances were controlled in the model by local blood flow rates. Since approximately 44% of the intracerebral resistance (25% of CVR) belongs to the capillaries and veins, which is approximately constant,[5] only the remaining 56% (32% of CVR) that belongs to the intracerebral arteries was allowed to change. In complete vasodilatation resistance of pial and intracerebral segments was allowed to decrease to 1/16 of the initial value which means a twofold increase in internal diameter. The resistance of large arteries was kept constant.

Assuming steady, laminar flow and writing linear pressure-flow relations for the 32 vessel segments and the appropriate flow balances for the 17 branch points, the system of 49 linear equations with 49 unknowns (32 flows, 17 pressures) was solved on digital computer. For the simulation of autoregulation an iterative procedure was used. Using the pressure and the flow values obtained from the previous solution of the equations, the appropriate segmental resistances were modified and used for the next approximation. The iterative solutions were always convergent within 10–15 steps.

In order to characterize the severity of cerebral ischemia in the areas having reduced blood flow, oxygen partial pressure in the tissue was calculated using a steady state Krogh cylinder model with concurrent flow. Neglecting axial diffusion, radial distribution of oxygen partial pressure in the tissue at each axial position along the capillary was calculated from the equations:

$$S = S_a - \frac{A(R_t^2 - R_c^2)}{K_1 R_c^2 v} z, \qquad (z = (O,L) \quad (1)$$

$$P_b = \left(\frac{K_2 S}{1 - S}\right)^{K_3}, \qquad (2)$$

$$P(r) = P_b - 2K_4 A R_t^2 (\ln r/R_c) + K_4 A(r^2 - R_c^2), \quad r = (R_c, R_t) \qquad (3)$$

where the following nomenclature has been used:
S = oxygen saturation of blood in the capillary
$S_a$ = arterial oxygen saturation
A = oxygen consumptiom in the gray matter
$R_t$ = radius of the oxygen consuming tissue cylinder
$R_c$ = capillary radius
v = average blood velocity
z = axial coordinate
L = capillary length
$P_b$ = average $pO_2$ in the blood
P(r) = $pO_2$ in the tissue at the radial coordinate r
$M_1 - K_4$ = constants

In the present calculations, resolution of 50 steps in the radial and 10 steps in the axial directions was used. In order to determine certain parameters of the model frequency distribution of $pO_2$ was generated using the calculated $pO_2$ values for normally perfused tissue and compared to a histogram of experimental data measured in the rabbit cortex.[9] Normal oxygen consumption and capillary length were obtained from the best fit of $pO_2$ histograms keeping the arterial and venous $pO_2$ at 95 and 35 mmHg, respectively (fig. 2). Other parameters were the same as used by Reneau et al.[10] Parameter values used for the present simulation are listed in table 2.

For normal flow the $pO_2$ was about 1 mmHg in the so-called lethal corner of the Krogh cylinder (fig. 3). Under ischemic conditions the oxygen consumption was assumed to follow zero order kinetics. That is, A was homogeneous and constant in the tissue cylinder except in the points were $pO_2$ was less than 1 mmHg, where A was set to zero. Accordingly, at each axial position $R_t$ was reduced to exclude the non-consuming tissue areas. The tissue $pO_2$ values were then recalculated and a new radial $R_t$ established. Final $pO_2$ distribution was obtained by repeating this procedure iteratively until the results became stable.

Figure 3 shows the shape and location of anoxic ($pO_2 < 1$ mmHg) areas in the Krogh cylinder at different reduced flow rates. The ITV (ischemic tissue volume) index was defined as the relative volume of the anoxic tissue. Although ITV was not related directly to the gross volume of ischemic brain tissue it was accepted as a local measure of the severity of ischemia.

## Results

Figure 4 shows cerebral autoregulation curves obtained by computer simulation. Since we were interested in hypotensive cases which accompany MCA occlusion, only the low pressure part of the autoregulation has been studied. The model demonstrates that the total cerebral blood flow (CBF) decreases when the arterial pressure is reduced below 60–70 mmHg. During unilateral occlusion of the MCA the autoregulation is partially damaged. Total CBF drops initially to 80–90% of the preocclusion value, which agrees well with the experimental findings.[11] With autoregulation, CBF reaches a slightly higher level. A leftward shift in the autoregulatory curve is also demonstrated, which occurs when maximum diameter of the pial arteries is increased twofold.

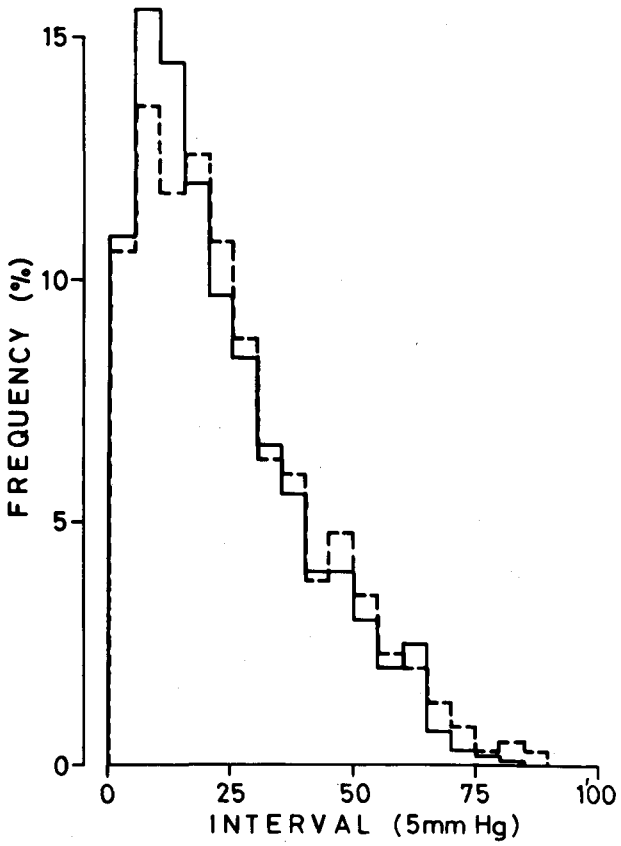


FIGURE 2. *Comparison of $pO_2$ histograms calculated using the Krogh cylinder model (solid line) and the measured data (dashed line) of Smith et al (1977).*

Regional autoregulation in the MCA territory is demonstrated in figure 5. Occlusion of the MCA leads to total disappearance of autoregulation in the ischemia area. Regional blood flow (rCBF) decreases to 42% of the preocclusion value at 120 mmHg mean arterial pressure. The post occlusion rCBF, however, depends largely on the actual diameter of the pial anastomoses. For example, if the anastomotic diameter varies over the range of 80–140 $\mu$m, blood flow in the MCA territory may decrease initially to 10–67% of the preocclusion value. Simultaneously, the ITV index varies in the interval of 2–40%, depending on the anastomotic diameter.

Influence of the actual anastomotic diameter on regional blood flow and oxygen supply in the specially important lenticulostriate area is demonstrated in figure 6. Oxygen supply is characterized by the average tissue $pO_2$ at the venous end of the Krogh cylinder —

TABLE 2 *Parameters of the Krogh Cylinder Model*

| | |
|---|---|
| $S_a$ = 0.9573 | $K_1$ = 0.204 |
| A = 19 × $10^{-4}$ ml·cm$^{-3}$·s$^{-1}$ | $K_2$ = $10^3$ |
| $R_t$ = 30 $\mu$m | $K_3$ = 0.4545 |
| $R_c$ = 2.5 $\mu$m | $K_4$ = 5.07 × $10^8$ |
| v = 0.004 cms$^{-1}$ | |
| L = 72 $\mu$m | |

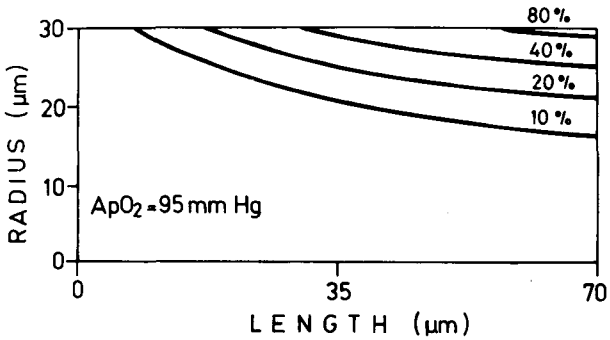


FIGURE 3. *Distribution of anoxic tissue ($pO_2$ < 1 mmHg) regions in the Krogh cylinder model at different reduced blood flow rates (10–80% of normal). $ApO_2$ = arterial oxygen partial pressure.*

as a representative value of tissue oxygenation in the weakly supplied microregions, and by the relative ischemic tissue volume (ITV). rCBF and this average $pO_2$ increases and ITV decreases with increasing anastomotic diameters during MCA occlusion. In addition, average $pO_2$ is a linear function of the anastomotic diameter with a correlation coefficient of 0.98. An anastomotic diameter of at least 170 $\mu$m is necessary to remove ischemia completely from the tissue.

Based on the hypothesis of long-term pial vascular adaptation in focal ischemia, further computer simulations were run to investigate the dependence of rCBF on the anastomotic diameter as a function of time elapsed from the beginning of the MCA occlusion. The mechanism of the adaptational process was presumed

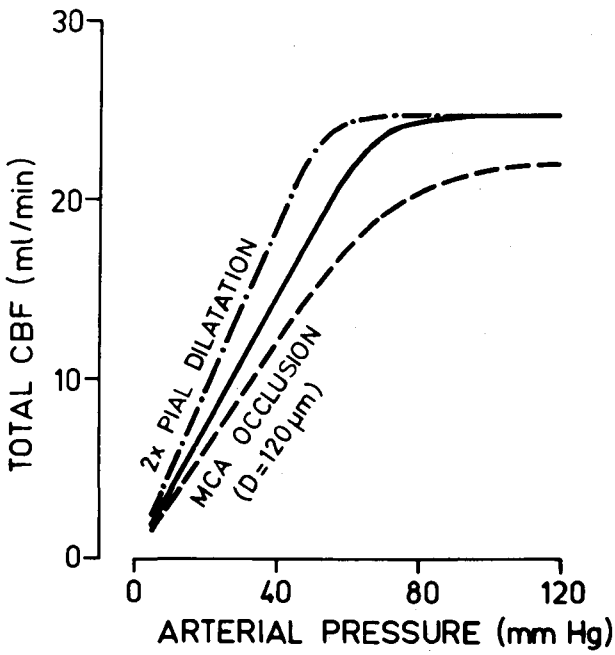


Figure 4. *Dependence of cerebral blood flow (CBF) on the arterial pressure as simulated by the computer model. The lower limit of normal autoregulation (solid line) is shifted to the left in case of chronic pial vasodilation. Autoregulation is weakened during occlusion of the middle cerebral artery. D = average anastomotic diameter.*

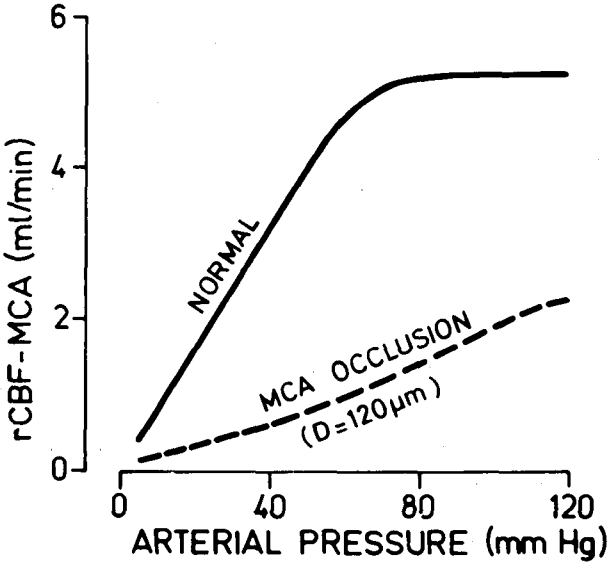


FIGURE 5. *Dependence of regional blood flow (rCBF) in the territory of the middle cerebral artery (MCA). Autoregulation is diminished in MCA occlusion in case of 120 μm average pial anastomotic diameter.*

to be an exponentially decelerating vasodilation:

$$R(t) = R_n + (R_o - R_n) \exp(-t/T), \quad (4)$$

where:
R(t) = pial anastomotic resistance at time t
$R_n$ = minimal anastomotic resistance
$R_o$ = R(0) at the time of occlusion
T = time constant of the adaptation.



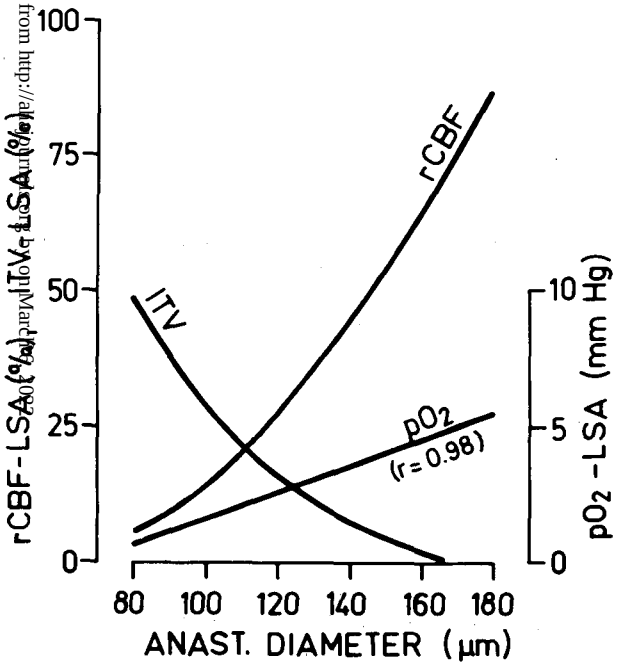


FIGURE 6. *Influence of the diameter of pial anastomoses on regional blood flow (rCBF), ischemic tissue volume (ITV) and average tissue oxygen partial pressure around the venous end of capillary ($pO_2$) in the lenticulostriate area (LSA) during occlusion of the middle cerebral artery.*

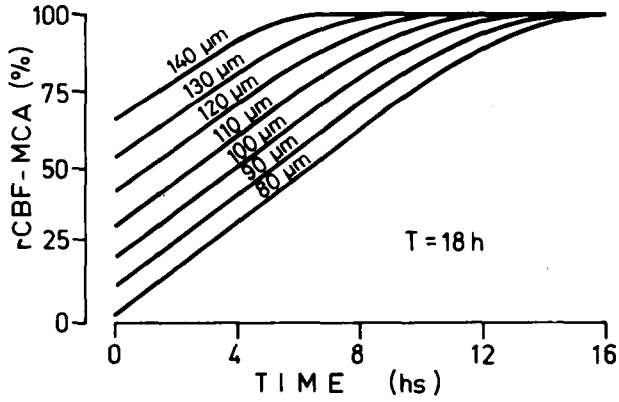


FIGURE 7. *Time course of equilibration of regional blood flow (rCBF) in the MCA territory in case of different anastomotic diameters from 80 to 140 μm. T = time constant of pial vascular adaptation.*

"The time constant of the adaptation was chosen as 18h and the minimal anastomotic resistance was calculated assuming a final (ie. fully "adapted") vessel diameter of 240 μm (for details see discussion)." Figure 7 demonstrates the influence of the initial anastomotic diameter on the equilibration time of rCBF in the ischemic MCA region. With an initial anastomotic diameter of 140 μm the equilibration time is 6–7 hours, while if the diameter is only 80 μm, the equilibration time can be as much as 16 hours.

In order to demonstrate intracerebral steal, vasodilator effect of high arterial $CO_2$ was simulated by the reduction of each postanastomotic segment to its minimum value. It was assumed that the anastomotic channels were already maximally dilated before the induced vasodilatation similarly to the intracerebral vessels in the ischemic MCA territory. Figure 8 shows that in case of anastomoses smaller than 200 μm blood flow is stolen from the ischemic area, while for greater anastomoses the general intracerebral vasodilation improves the blood flow in the same region.

Based on the pial vascular adaptation defined by eq. (4), computer simulation predicts the time course of steal reversal as shown in figure 9. Immediately after the occlusion, intracerebral vasodilation evokes approximately 30% steal of blood flow from the ischemic MCA territory (initial anastomotic diameter = 120 μm). Intracerebral steal disappears and reverses 16–24 hours later (20 hs if the initial anast. diam. = 120 μm). After 36 hours blood flow increases by 15–20% in response to intracerebral vasodilation.

## Discussion

Since the first attempt to model the hemodynamics of the circle of Willis by rigid plastic tubes,[12] several physical,[13, 14] electrical,[15, 16] and more advanced computer models[17, 18, 19] have been developed to simulate steady and pulsatile flow in the major cerebral arteries. In case of the occlusion of the MCA, however, the circle of Willis is of less significance because collateral circulation in the ischemic territory can be established through the pial anastomoses only. Since we have been

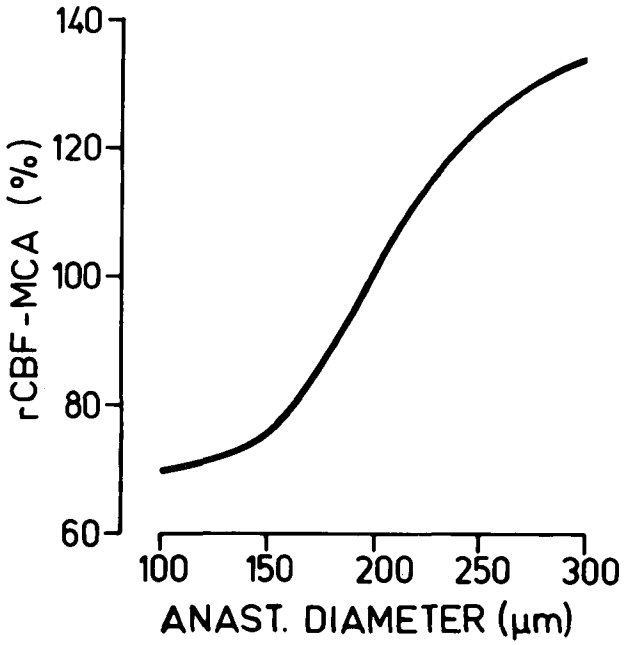


FIGURE 8. *Dependence of intracerebral steal of regional blood flow (rCBF) in the MCA territory on the actual diameter of pial anastomoses. rCBF was plotted as percent of the flow values preceding the intracerebral vasodilation.*

interested primarily in the computer simulation of focal cerebral ischemia in response to MCA occlusion, the pial anastomoses connecting the branches of the anterior and the posterior cerebral artery with those of the middle cerebral artery were included as an essential component of the present cerebral circulation model.

Likewise, none of the above mentioned models have attempted to simulate cerebral autoregulation. Our preliminary studies revealed, however, that active alterations in the preanastomotic and postanastomotic arterial diameters may affect the pial collateral flow

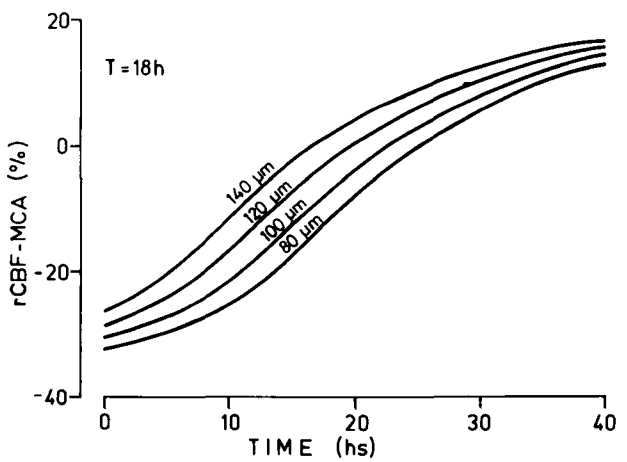


FIGURE 9. *Dependence of regional blood flow (rCBF) in the MCA territory on the time elapsed from the onset of MCA occlusion in case of different pial anastomotic diameters (80–140 μm). The difference between rCBF before and after intracerebral vasodilatation was plotted as a function of occlusive tissue.*

critically. Therefore, regional autoregulation was included in the present model. Autoregulation was represented as local pressure and flow control in the pial and intracerebral arteries, respectively. Although there is still controversy in the literature about the role of different local neural and humoral factors in cerebral autoregulation, the above scheme of segmental control seems to be justified.[5]

The integral control of pressure and flow used in the present model was an obvious oversimplification of the real cerebral autoregulation. Pressure at the pial anastomoses was kept constant until the preanastomotic resistance was reduced to minimum in contrast to the observation that pial artery pressure changes with the systemic pressure.[5] Also, cerebrovascular resistance was constant below 50 mmHg in Figure 4 due to the maximal dilatation of both pial and intracerebral arteries, although cerebral arterioles were known to continue to dilate to pressures as low as 35 mmHg.[20] However, in order to simulate the plateau and lower limit of the cerebral autoregulation the simplified scheme used for the control was satisfactory in the present model. The actual mechanism of pressure and flow regulation were not defined explicitly in the model. Overall cerebral autoregulation has been successfully simulated using $pO_2$, $pCO_2$, and pH as control signals,[21] however, without knowing the specific segmental action sites of the controlling factors, their incorporation into a regional regulatory model was not reasonable. Nevertheless, the present mathematical model was able to simulate quasi-normal cerebral autoregulation (at least below 120 mmHg), autoregulatory shift in response to chronic dilation of the pial vasculature and disturbance of autoregulation during arterial occlusion.[22] Since the gain of vascular control was not allowed to change in the model, this suggests that the breakdown of normal autoregulation is not necessarily related to reduced responsiveness of the cerebral arteries, but may be at least in part the consequence of the maximum dilation of the arterial vasculature in the ischemic area.

In addition to the calculation of regional blood flow, the Krogh cylinder model made it possible to estimate the severity of ischemia by calculating the $pO_2$ distribution and the anoxic "microvolume" of a representative tissue cylinder. As a result of fitting the $pO_2$ frequency distribution to the measured data a very low $pO_2$ value, about 1 mmHg, was obtained in the lethal corner of the Krogh cylinder for normally perfused tissue. In accordance with the low $pO_2$ values the figure for normal oxygen consumption obtained from the best fit of the histograms was about two times higher than the figure ($8.34 \times 10^{-4}$ mlcm$^{-3}$s$^{-1}$) used by Reneau et al.[10] for cerebral gray matter. Also, the capillary length of 72 μm instead of 180 μm was obtained. This shorter average length of capillaries was confirmed by our recent morphologic studies on the cortex of monkey brains perfused with India ink after formalin fixation (unpublished). Regarding the figure obtained for the oxygen consumption, it cannot be excluded that a more sophisticated $pO_2$ model, such as the Krogh cylinder with countercurrent instead of concurrent flow,

might have predicted a lower consumption value with an equaly good fit to the same $pO_2$ histogram.

Results of the present computer simulation have emphasized the importance of pial anastomoses in determining regional blood flow and oxygen supply of the ischemic cerebral tissue and thus the outcome of the ischemic cerebral injury in response to the occlusion of the middle cerebral artery. According to Blinkov and Glezer,[6] large pial anastomoses of the monkey brain average 120 $\mu$m in diameter. This value gave 58% reduction in CBF in response to MCA occlusion. It is important to remember here, however, that only a virtual length was assigned to the anastomotic segments in the model. Pial anastomoses form a complex arterial network on the surface of the brain, a definite length thus could not be established. On the other hand, it was possible to estimate the overall hydrodynamic resistance of the anastomotic connections by comparing computer simulation results to experimentally measured data. Pial arterial pressure was found to decrease to 10–30 mmHg,[23] or 20–30% of normal during MCA occlusion in the macaque.[24] After adjusting the anastomotic resistance to the appropriate value, the model predicted a pial arterial pressure of 10–16 mmHg (18–32% of normal) in simulated MCA occlusion. Using the obtained anastomotic resistance and 120 $\mu$m for the anastomotic diameter, a virtual length of 3.5 mm was calculated and used for the computer simulation.

It is not only the anatomical variability of the diameter of anastomoses that we must consider but, also as we have mentioned earlier, a long-term adaptation of the pial vasculature. That is, if the pial arteries and anastomoses dilate to a certain extent during chronic MCA occlusion, regional and total CBF can be restored over a period of time. This does not occur necessarily in all experimental cases, but an approximate characteristic time of the flow restoration of 12 hours can be presumed.[3] Supposedly, the vasodilatation in the ischemic region does not stop when the blood flow reaches the preocclusion value, but the process continues until the autoregulatory capacity is liberated and restored in that area. It is not possible to determine theoretically the limit of the adaptation, and the individual variation seems to be also rather large. Therefore, as a first approximation it was assumed that the arterial dilatation comes to a stop when the hemodynamics and autoregulation are completely restored in the previously ischemic area. In the present mathematical model a twofold increase in the pial arterial diameter with an initial anastomotic diameter of 120 $\mu$m was necessary to achieve complete restoration of autoregulation. This means that the final anastomotic diameter should be about 240 $\mu$m. Then, if the vascular adaptation is an exponentially decelerating process as a first approximation, the 12 h flow equilibration with the 240 $\mu$m final anastomotic diameter gives T = 18 h for the time constant. Using these figures, the computer simulation predicted an equilibration time of 6–16 hours if the anastomotic diameter varied in the interval of 80–140 $\mu$m. If not, only the initial anastomotic diameter but also the time constants of the adaptational process are different in each individual case, variation in the equilibration time can be even greater. Of course, the time course of pial vascular adaptation should be determined experimentally before conclusions can be drawn for the real cerebral circulation. Also, anastomoses of relatively small size may not always reach the maximal value of 240 $\mu$m *in vito*. With the development of cerebral edema following MCA occlusion and consequent increase in intracranial pressure,[2] the degree of cerebrovascular resistance at the capillary and venous levels will probably increase which may compromise the collateral circulation to the ischemic region and reduce the adaptational capacity of the pial vasculature. Consideration of such changes which are in competition with the adaptational process will be the subject of future improvement of the present hemodynamic model.

The present simulation predicts that pial arterial constriction in chronic hypertension would result in a larger volume of ischemia initially, as well as a longer time for adaptation of the collateral circulation, both of these resulting in a more severe clinical outcome. This is consistent with our recent experiments in the spontaneously hypertensive rat in which previously treated rats tolerated cerebral ischemia better than did untreated animals with the same arterial occlusion.[25]

The model was also able to simulate intracerebral steal and inverse steal. These phenomena can be elicited experimentally by a strong vasodilator, like high arterial $pCO_2$. Since $CO_2$ acts primarily on the small cerebral vessels,[26] and pial arterioles of similar size,[27] the effect of $CO_2$ was simulated by maximal dilatation of the postanastomotic arterial segments. The present results suggest that the reversal of intracerebral steal can indeed be explained by the chronic dilation of the pial arteries including the pial anastomoses. With an initial anastomotic diameter of 120 $\mu$m a twofold increase in the pial diameters produced 20% increase in rCBF in response to acute intracerebral vasodilation during MCA occlusion. Recalling that the same extent of pial arterial dilation lowered the limit of autoregulation by 30–40 mmHg (fig. 3), this suggests that both the steal reversal and the autoregulatory shift can be the consequence of a chronic pial vascular adaptation in long-term cerebral ischemia.



## Acknowledgments

The authors express their thanks and appreciation to Prof. A.G.B. Kovach for supporting this work and to Dr. R.W. Schubert for the useful suggestions in oxygen transport.

## References

1. Halsey JH, Capra NF: Physiological modification of immediate ischemia due to experimental middle occlusion and its relevance to cerebral infarction. Stroke **2:** 239–246, 1971
2. Halsey JH, Capra NF: The course of experimental cerebral infarction — the development of increased intracranial pressure. Stroke **3:** 268–278, 1972
3. Halsey JH, Clark LC: Some regional circulatory abnormalities following experimental cerebral infarction. Neurology **20:** 238–246, 1970
4. Meyer J, Denny Brown D: The cerebral collateral circulation. Neurology **7:** 447–458, 1957

5. Kontos HA, Wei EP, Navari RM, Levasseur JE, Rosenblum WI, Patterson JL: Responses of cerebral arteries and arterioles to acute hypotension and hypertension. Am J Physiol **234:** H371–H383, 1978
6. Blinkov SM, Glezer II: The human brain in figures and tables. New York: Plenum Press, 1968
7. Heistad DD, Marcus ML, Abboud FM: Role of large arteries in regulation of cerebral blood flow in dogs. J Clin Invest **62:** 761–768, 1978
8. Johnson PC: Myogenic tone in resistance vessels. In Mechanism of Vasodilation. Satellite Symp 27th Int Congr Physiol Sci, Wilrijk 1977, pp. 73–78. Basel: Karger, 1978
9. Smith RH, Gilbeau EJ, Reneau DD: The oxygen tension field within a discrete volume of cerebral cortex. Microvascular Res **13:** 233–240, 1977
10. Reneau DD, Bruley EF, Knisley MH: A computer simulation for prediction of oxygen limitations in cerebral gray matter. J Assoc Advance Med Inst **4:** 211–223, 1970
11. Morawetz RB, DeGirolami U, Ojemann RG, Marcoux FW, Crowell RM: Cerebral blood flow determined by hydrogen clearance during middle cerebral artery occlusion in unanesthetized monkeys. Stroke **9:** 143–149, 1978
12. Avman N, Bering EA: A plastic model for the study of pressure changes in the circle of Willis and major cerebral arteries following arterial occlusion. J Neurosurg **18:** 361–365, 1961
13. Himwich WA, Knapp FM, Weinglarz RA, Martin JD, Clark MD: The Circle of Willis as simulated by an engineering model. Arch Neurol **13:** 164–172, 1965
14. Himwich WA, Clark ME: Simulation of flow and pressure distributions in the Circle of Willis. *In* Pathology of Cerebral Microcirculation, J. Corvas-Navarro (Ed.), New York: Walter de Gruyter, pp. 140–152, 1974
15. Murray KD: Dimensions of the Circle of Willis and dynamic studies using electrical analogy. J Neurosurg 21: 26–34, 1964
16. Clark ME, Martin JD, Wenglarz RA, Himwich WA, Knapp FM: Engineering analysis of the hemodynamics of the circle of Willis. Arch Neurol **13:** 173–182, 1965
17. Chao JC, Hwang NHC: A dynamic model of the circle of Willis. J Biomechanics **4:** 141–147, 1971
18. Clark ME, Kufahl RH: Simulation of the cerebral macrocirculation. *In* Cardiovascular System Dynamics. J Baan, A Noordegraaf, J Raines (Eds.), Cambridge, Massachusetts: MIT Press, pp. 380–390, 1978
19. Austin GM: Prediction of relative flow deficit and EC-IC effectiveness by computer model of the circle of Willis. J Cerebral Blood Flow and Metabolism **1** (Suppl 1), S497–S498, 1981
20. MacKenzie ET, Farrar JK, Fitch W, Graham DI, Gregory PC, Harper AM: Effects of hemorrhagic hypotension on the cerebral circulation I. Cerebral blood flow and pial arteriolar caliber. Stroke **10:** 711–718, 1979
21. Greenberg JH, Noordegraaf A, Reivich M: Control of cerebral blood flow: model and experiments. *In* Cardiovascular System Dynamics, J Baan, A Noordegraaf, J Raines (Eds.), Cambridge, Massachusetts: MIT Press, pp. 291–299, 1978
22. Symon L, Branston NM, Strong AJ: Autoregulation in acute focal ischemia: an experimental study. Stroke **7:** 547–554, 1976
23. Symon L, Ishikawa S, Meyer JS: Cerebral arterial pressure changes and development of leptomeningeal collateral circulation. Neurology **13:** 237–250, 1963
24. Symon L: A comparative study of middle cerebral pressure in dogs and macaques. J Physiol **191:** 449–465, 1967
25. Halsey J, O'Brien M, Strong E: Amelioration of cerebral ischemia by prior treatment of hypertension. Stroke **11:** 235–240, 1980
26. Kontos HA, Wei EP, Raper AJ, Patterson JL: Local mechanism of $CO_2$ action on cat pial arterioles. Stroke **8:** 226–229, 1977
27. Wei EP, Kontos HA, Patterson JL: Dependence of pial arteriolar response to hypercapnia on vessel size. Am J Physiol **238:** H697–H703, 1980